



Removal of safranin O from wastewater using *Streptomyces griseobrunneus* dead biomass and in silico calculations

Muhammed Safa Çelik¹ · Nurşah Kütük² · Ali Fazıl Yenidünya¹ · Serap Çetinkaya¹ · Burak Tüzün³

Received: 1 May 2023 / Revised: 22 June 2023 / Accepted: 25 June 2023

© The Author(s), under exclusive licence to Springer-Verlag GmbH Germany, part of Springer Nature 2023

Abstract

Environmental pollution with the dye produced by the textile industry causes a serious problem worldwide. The aim of the study is to use the environmentally friendly and low-cost *Streptomyces griseobrunneus* (*S. griseus* S15) dead cells for the adsorption of safranin O from aqueous milieu. Optimum retention was achieved with 200 mg/L safranin O and 25 g/L adsorbent at pH 9. Biosorption was found to better fit the Langmuir isotherm and PSO kinetics. The maximum biosorption (q_{\max}) was 188.67 mg/g. The reaction between *S. griseus* S15 and safranin O was chemical, exothermic, and spontaneous. *S. griseus* S15 biomass was reusable. Molecules supposed to be involved in the process were investigated by using a Gaussian software program, calculations B3LYP, HF, and M06-2X, 6-31G, 6-31++G, and 6-31++G**. For molecular docking calculations, the affinity of safranin O molecule to various proteins was investigated. Finally, ADME/T was applied to gain an insight into the possible effects of safranin O on human health.

Keywords Biosorption · In silico · Safranin O · *Streptomyces griseobrunneus* · Wastewater

1 Introduction

Textile industry alone constitutes nearly one-seventh of the total world manufacture [1]. It is also one of the foremost freshwater consumers, making it a heavily polluted wastewater discharger. Many of the dyes ending up in wastewater have global detrimental consequences [2–4]. The elimination of dyes from industrial vents has therefore been given a substantial consideration [5], and a wealth of data have been made available [6–8]. For the most part, the treatment of textile wastewater is based on processes that were helpful up to a certain point [9] as the cost of the treatment processes and large quantities of by-products produced have been posing other problems [10]. To this end, the biological adsorption has been thought to provide better means to tackle

such complications [11, 12]. It is a relatively inexpensive approach compared to other physical and chemical treatments [13], and dead or alive fungal and bacterial adsorption has been widely exploited in wastewater management [12–15]. Live cells bind the positively charged dye particles on the cell-wall surface thanks to the presence of negatively charged polysaccharides, proteins, and lipids in Fig. 1 [12].

Biosorbents are the cost-effective versatile materials for the removal of toxic pollutants or for the recovery of valuable ions from aqueous wastewater [16–19]. The main advantages of this technology over conventional technologies include ability to regenerate, high efficiency, sludge minimization [7].

It could be emphasized that using bacteria as a precursor for the bioremediation of dyes yields better results in a wide variety of procedures and conditions [20, 21]. Bacterial strains are capable of reducing and converting many toxic compounds into non-toxic end-products [22]. Many bacterial species have been exploited for decolorization of wastewater and dye degradation [23, 24].

Actinobacteria are metabolically diverse Gram-positive microorganisms. They share some morphological properties with both bacteria and fungi [25]. *Streptomyces*, an actinobacterial genus, comprises majority of the antibiotic producing species [26]. They breakdown cellulose and produce humus.

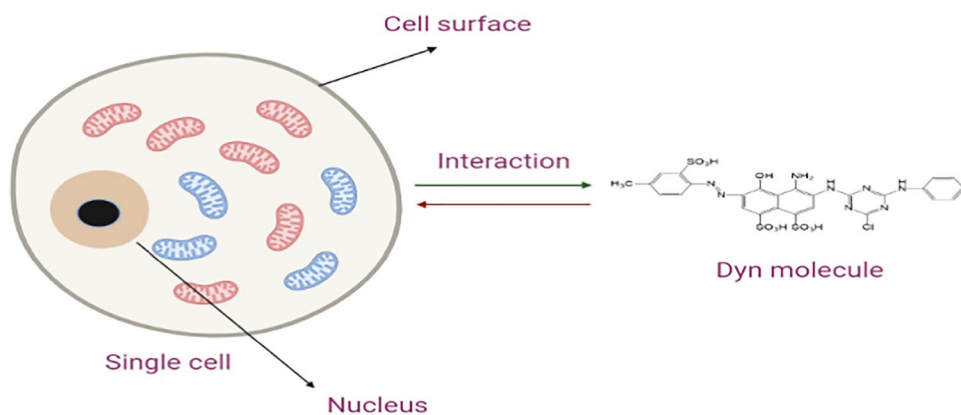
✉ Burak Tüzün
theburaktuzun@yahoo.com

¹ Department of Molecular Biology and Genetics, Science Faculty, Sivas Cumhuriyet University, Sivas, Turkey

² Department of Chemical Engineering, Faculty of Engineering, Sivas Cumhuriyet University, Sivas, Turkey

³ Plant and Animal Production Department, Technical Sciences Vocational School of Sivas, Sivas Cumhuriyet University, Sivas, Turkey

Fig. 1 Interaction of dye and microbial cell



Created in BioRender.com

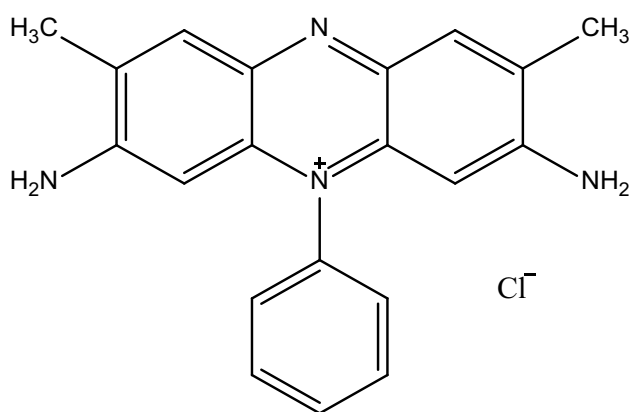


Fig. 2 Chemical structure of safranin O

Furthermore, several species of this genus have the ability to use paint contaminants as the sole carbon source [27, 28].

Bacteria possess two types of cell wall, gram-positive with a thick cell surface peptidoglycan layer connected by amino acid bridges, and gram-negative, consisting of a relatively much thinner (10–20%) peptidoglycan layer, complexed with phospholipids and lipopolysaccharides.

Recent studies have demonstrated that theoretical calculations become very important in many stages from synthesis and characterization to activity comparison [28]. Gaussian software and Maestro Schrödinger are the most widely used and known among these [29–31]. Chemical quantum properties of polluting molecules can provide important clues as to their interactions with the molecules of biosorbent [32], using the Maestro Schrödinger program. ADME/T calculations are often performed with the same program to envisage the effects, reactions, and movements of molecules in human metabolism.

Safranin O is a cationic salt in Fig. 2. The structural complexity and stability of the safranin create problems during its biodegradation [33]. This dye can damage

nucleic acids and disposes humans to carcinogenicity. Environmentally friendly and cost-effective *S. griseus* S15 dead cells were preferred for the adsorption of safranin O from the aqueous medium. Factors affecting biosorption, namely pH, biosorbent dose, initial dye concentration, adsorption kinetics as well as desorption capacity and reusability were investigated. Molecular docking was employed to examine the interaction between the safranin O and the bioadsorbent.

2 Experimental sections

2.1 Materials

Safranin O, ethanol (EtOH), hydrochloric acid (HCl), sodium hydroxide (NaOH) used in the experiments were of analytical purity and obtained from Merck and Sigma-Aldrich companies.

2.2 Biosorbent characterization

Functional groups on the biosorbent surface were explored by Fourier Transform Infrared (FTIR) Spectrometer (ATR, Bruker, Tensor II) before and after biosorption. Its surface morphology was imaged by scanning electron microscopy (SEM) (TESCAN MIRA3 XMU) at CÜTAM Central Laboratory of Sivas Cumhuriyet University, Turkey.

2.3 Preparation of the biosorbent

In the biosorption of safranin O on bacterial biomass, *Streptomyces griseobrunneus*, previously isolated from soil [34], was used (GenBank Accession Number: MW077440). *S. griseus* S15 was obtained in LB culture in a 250 mL, 500 mL vessel, for 24h by shaking at 150

rpm at 37°C. Cells were weighed [35] after precipitating for 10 min at 5000 rpm (Eppendorf 128 5804, Germany) and dried for 24h at 40°C.

2.4 Adsorption reaction

Safranin O, 1000 ppm, was dissolved in deionized water, and this stock solution was used in the 24-h adsorption reaction, 10 mL. The reaction conditions were as follows: reaction temperature, 25°C; biosorbent, 50 mg; pH range 1, 3, 5, 7, 9, and 11. The reaction mixture was agitated by shaking. pH was adjusted with 0.01M HCl or NaOH. In kinetic experiments, varying dye concentrations, between 30 and 250 mg/L, and time intervals, between 10 and 1440 min, were employed. The biosorbent was precipitated by centrifugation [36, 37], and unbound dye was estimated at 520 nm.

The biosorption efficiency was calculated with Eq. 1, below. The biosorption capacity (q_e) of biosorbent was calculated with Eqs. 2 and 3.

$$\% \text{Biosorption efficiency} = \frac{C_0 - C}{C_0} \times 100 \quad (1)$$

$$q_e = \frac{(C_0 - C_e) \cdot V}{m} \quad (2)$$

$$q_t = \frac{((C_0 - C_t) \cdot V)}{m} \quad (3)$$

C_0 , the initial dye concentration (mg/L); C , the dye concentration (mg/L) at time t ; q_e , the biosorption capacity (mg/g) at equilibrium; q_t , the biosorption capacity (mg/g) at $t = t$; C_e , the final concentration (mg/L); V , the solution volume (mL); and m , the biosorbent amount (g).

2.5 Recovery studies

Three different tubes were taken and labeled, EtOH, HCl, NaOH, into which dye solution and 50 mg of sample were added and incubated for 24h. Three-milliliter solutions were saved, and the remainder was centrifuged. Onto the pellets, 10 ml of either of 0.1 M HCl, EtOH, NaOH was added and washed for 15 min. This process was repeated once more. The pellets were likewise washed with dH₂O. Samples taken as equilibrium 1, 2, 3, 4, 5 were measured in a spectrophotometer at 520 nm. % Desorption was calculated by Eq. 4 [38].

$$\text{Desorption}\% = \frac{Q_{des}}{Q_{ads}} \times 100 \quad (4)$$

Q_{ads} , dye adsorbed (mg/g), and Q_{des} , desorbed dye (mg/g).

2.6 Theoretical methods

Hypothetical assessments yield significant data on the functional aspects of molecules. Numerous chemical quantum factors can be included into t . The calculated parameters were used to explain the chemical activities of the molecules. Gaussian09 RevD.01 and GaussView 6.0 [39, 40] software was employed, and assessments were obtained in B3LYP, HF, and M06-2x with 6-31G, 6-31++G, and 6-31++G** basis set [41, 42].

$$\chi = -\left(\frac{\partial E}{\partial N}\right)_{v(r)} = \frac{1}{2}(I + A) \cong -\frac{1}{2}(E_{HOMO} + E_{LUMO}) \quad (5)$$

$$\eta = -\left(\frac{\partial^2 E}{\partial N^2}\right)_{v(r)} = \frac{1}{2}(I - A) \cong -\frac{1}{2}(E_{HOMO} - E_{LUMO}) \quad (6)$$

$$\sigma = 1/\eta \quad \omega = \chi^2/2\eta \quad \varepsilon = 1/\omega \quad (7)$$

An important method used to determine the molecules with the highest activity against biological materials is molecular docking. Molecular docking calculations were performed in Schrödinger's Maestro Molecular modeling platform (version 12.8) [43]. The calculations give information on the active groups of molecules. Calculations included several modules, the first of which was the protein preparation module [44]. The second step involved the LigPrep module [45]. Glide ligand docking step involved the interaction taken place between proteins and other molecules [46]. Finally, the Qik-prop module of the Schrödinger software [47] was used to perform ADME/T analysis (absorption, distribution, metabolism, excretion, and toxicity) in order to predict the effects of the molecules on human metabolism.

3 Results and discussions

3.1 Structural analyses of the biosorbent

3.1.1 FTIR analysis

FTIR spectra of *S. griseus* S15 were obtained before and after safranin O biosorption (Fig. 3). The broad peak at approximately 3271 cm⁻¹ signified the O–H bond and N–H band [48, 49]. A C–H asymmetric stretch was identified at 2922 cm⁻¹ [34]. An aromatic ring stretching vibration was observed at 1633 cm⁻¹, while a CH₃ stretching vibration was found at 1452 cm⁻¹. An aromatic C=N stretching vibration was seen at 1397 cm⁻¹. The aromatic C=N stretching vibration of the chromophore of safranin O was detected at 1394 cm⁻¹ [50]. A C–H bond vibration was indicated at

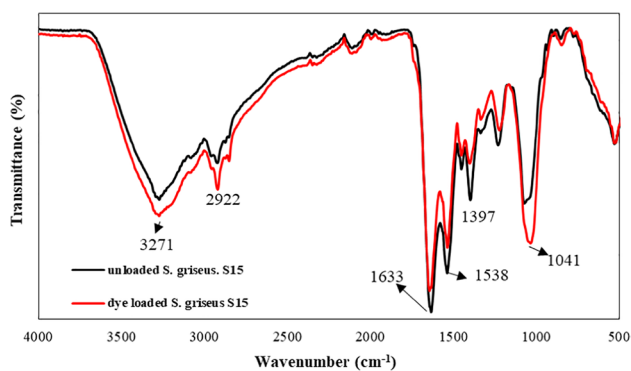


Fig. 3 FTIR spectra of before and after biosorption

1041 cm^{-1} [51]. The intensity of some peaks decreased or increased after adsorption, indicating that the dye molecules were specifically loaded on the bioadsorbent via hydrogen bonding or electrostatic attractions [51, 52].

Fig. 4 SEM images of *S. griseus* S15 before (a) and after biosorption (b)

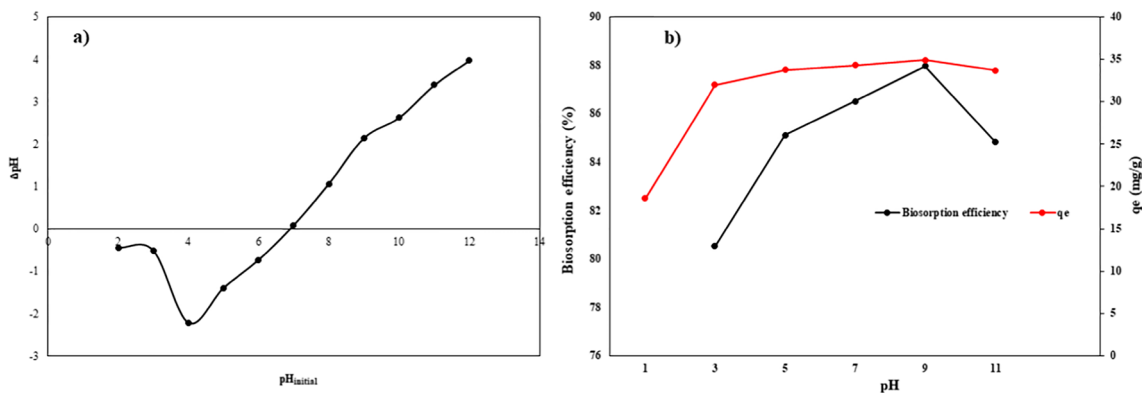
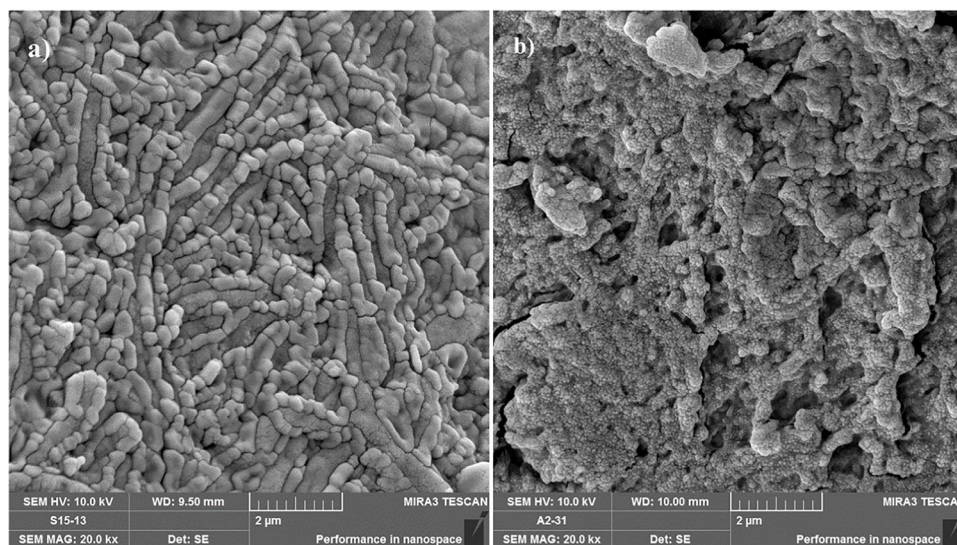


Fig. 5 Effect of solution pH on biosorption (%) (a) and q_e (b)

3.1.2 SEM analysis

The surface properties of the *S. griseus* S15 were examined by SEM before and after safranin O biosorption in Fig. 4a, b, respectively. *S. griseus* S15 appeared to be swollen after adsorption. Hence, distinct round, ellipsoidal, and wavy structures, in Fig. 4a, became fuzzy and less distinct in Fig. 4b [53].

3.2 Biosorption procedure

3.2.1 The role of pH

pH is a key factor since it disturbs the surface charges of both the adsorbent and dye [52]. In this study, the zero-point charge (pH_{pzc}) of the biosorbent was investigated by keeping the initial pH value of the solution within 2 and 12, with 0.1 M KNO_3 in Fig. 5a. The pH_{pzc} value was determined at 6.89, indicating that the amount of negative charge of the

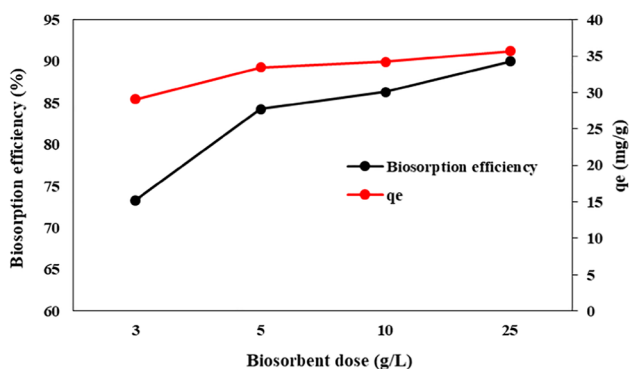


Fig. 6 Effect of biosorbent dose on biosorption efficiency and q_e

biosorbent surface increased at pH points above the pH_{pzc} value [52].

The role of pH on the adsorption was investigated in Fig. 5b. The highest biosorption efficiency, 88%, was achieved at pH 9 where biosorption capacity was calculated to be 34.8 mg/g. It was evidenced that both the efficiency and capacity of biosorption increased in elevated levels of OH^- on the biosorbent surface, enabling an electrostatic interaction with the cationic safranin O [49]. Expectedly, after reaching a certain pH point, biosorption efficiency started to decrease. Two possible explanations were made for this phenomenon: (1) the solubility of the dye increased at high pH, and the adsorption decreased; (2) at high pH, safranin O started to lose protons and, as a consequence, the electrostatic interaction decreased [54].

3.2.2 Biosorbent concentration

Biosorbent dose is an important parameter affecting biosorption [51]. The effect of biosorbent dose on biosorption was investigated in the range of 3 g/L and 25 g/L, keeping the initial dye concentration constant in Fig. 6. It could be seen

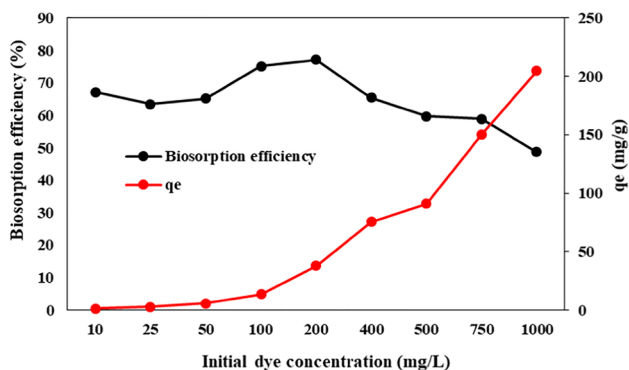


Fig. 7 The role of initial dye concentration on biosorption efficiency and q_e

that the biosorption efficiency and biosorption capacity steadily increased in proportional to biosorbent dose. This can be caused by the agglomeration of some dye molecules on the biosorbent surface [55] or due to the overlapping of the biosorption sites [52].

3.2.3 Role of dye concentration

The effect of the initial dye concentration on the biosorption was investigated at safranin O concentrations ranging from 10 to 1000 mgL^{-1} in Fig. 7. After around 200 mg/g , the biosorption efficiency decreased. After a certain concentration, the active sites on the biosorbent surface reached saturation [52]. The highest biosorption efficiency, 77%, was obtained with 200 mgL^{-1} safranin O and 5 mgL^{-1} biosorbent dose.

The Langmuir isotherm (Eq. 8) indicates homogeneous biosorbent structure and the presence of monolayer biosorption. Freundlich isotherm expresses heterogeneous biosorbent surface and multilayer biosorption (Eq. 9). Temkin isotherm expresses the energy and heat distribution between sorbent and sorbate (Eq. 10). K_L (mgL^{-1}), Langmuir constant; K_f , Freundlich constant; n Freundlich isotherm constant; q_{max} , maximum biosorbent capacity; K_T , the constant of the Temkin isotherm; β , the constant related to the heat of biosorption. If Freundlich isotherm constant value, n , is 0, the process is linear; if less than 1, the process is physical; and if greater than 1, the process is chemical.

$$\frac{1}{q_e} = \frac{1}{q_{max}} + \left(\frac{1}{K_L \cdot q_{max}} \right) \left(\frac{1}{C_e} \right) \tag{8}$$

$$\ln q_e = \ln K_f + \left(\frac{1}{n} \right) \ln C_e \tag{9}$$

$$q_e = \beta \cdot \ln K_T + \beta \cdot \ln C_e \tag{10}$$

Table 1 Data of isotherm models

Isotherm model	Value
Langmuir	
R^2	0.98
K_L (L/g)	0.00215
q_{max} (mg/g)	188.67
Freundlich	
R^2	0.89
$1/n$	0.8165
K_f (L/g)	0.68
Temkin	
R^2	0.73
K_T (L/g)	7.515
β	18.257

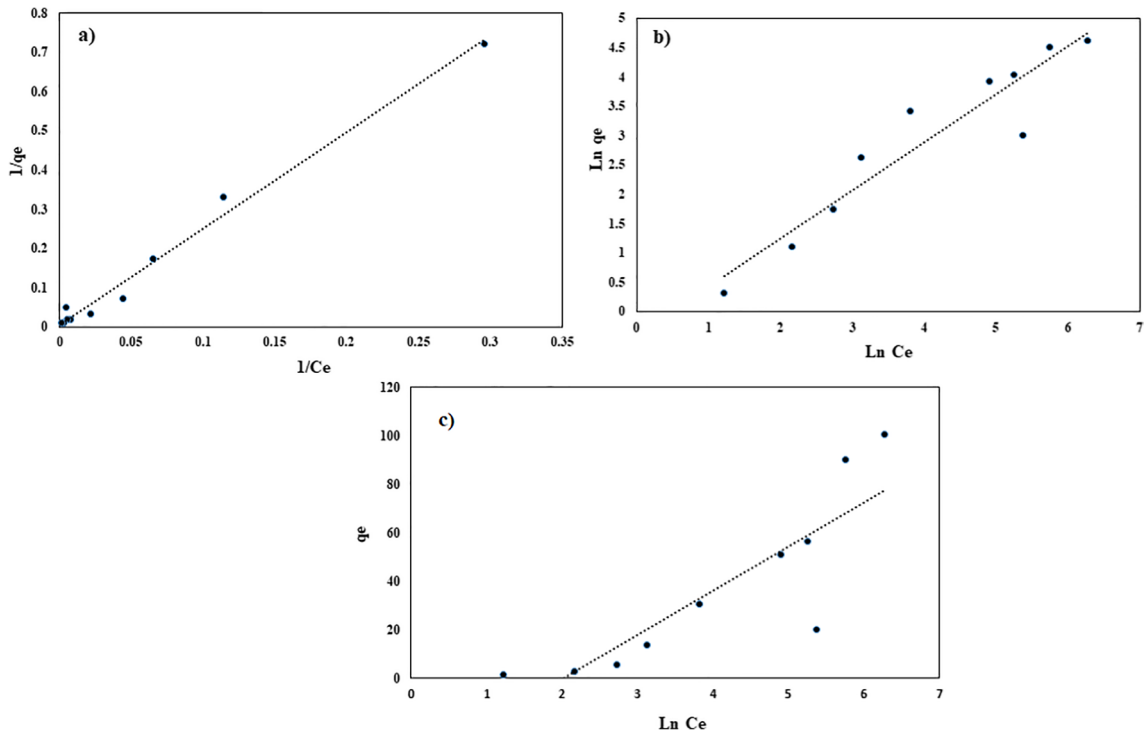


Fig. 8 Isotherm models: a) Langmuir, b) Freundlich, and c) Temkin

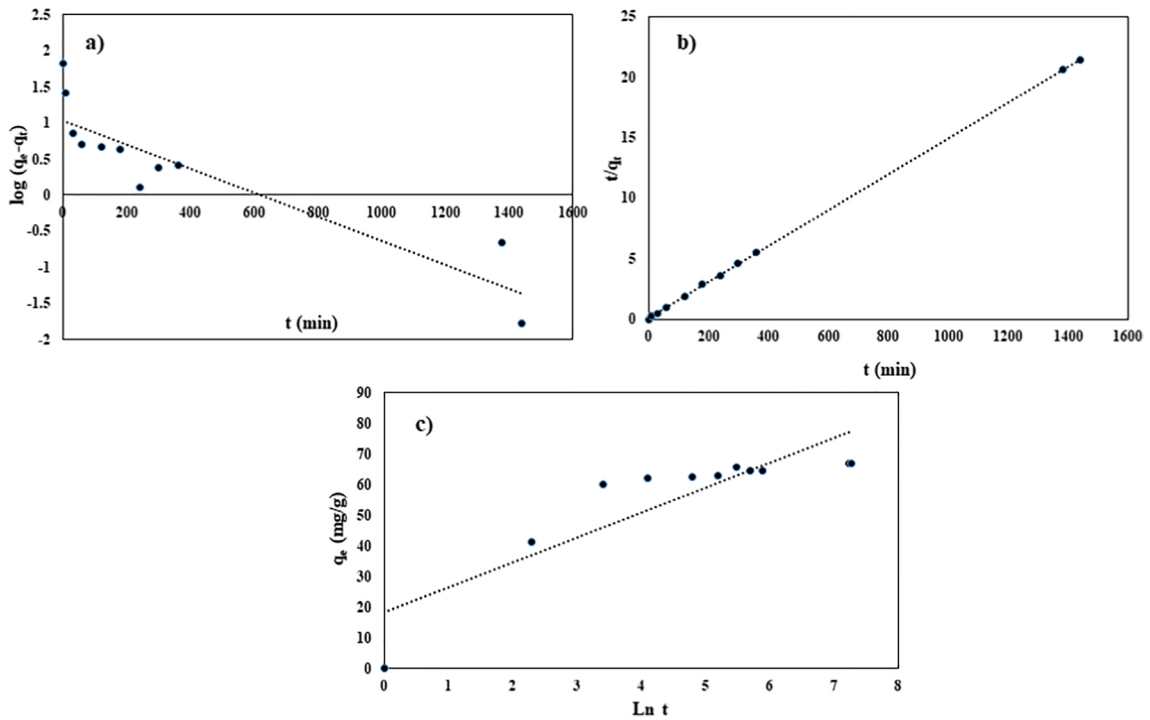


Fig. 9 Kinetic models: a) PFO, b) PSO, and c) Elovich model

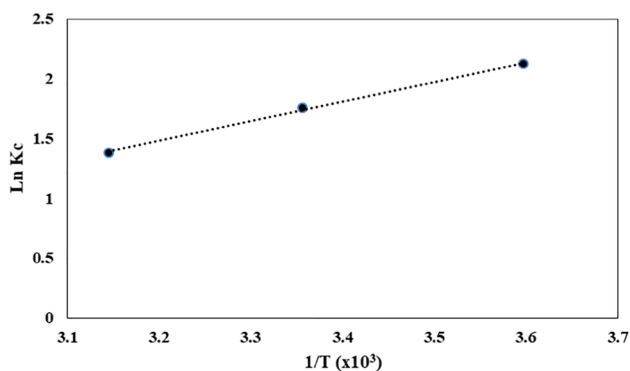


Fig. 10 Biosorption thermodynamic (C_o : 200 mg/L, m : 50 mg, temperature: 25 °C, contact time: 24 h)

Langmuir isotherm, q_{max} and K_L , were calculated to be 188.67 mg/g and 0.00215 L/g, respectively in Table 1. The highest Langmuir isotherm was $R^2=0.98$ in Fig. 8. This result indicated that the safranin O was absorbed as an even monolayer [48, 56].

3.2.4 Kinetic calculations

To better understand the biosorption mechanism, reaction kinetics were investigated using pseudo-first-order (PFO, Eq. 11), pseudo-second-order (PSO, Eq. 12), and Elovich models in Fig. 9 (Eq. 13). Here, k_2 is the reaction constant for PSO, and α and β are Elovich model constants.

$$\log(q_e - q_t) = \log q_e - \frac{k_1}{2.303} t \tag{11}$$

$$\frac{t}{q_t} = \frac{1}{k_2 \cdot q_e^2} + \frac{1}{q_e} t \tag{12}$$

$$q_t = \frac{1}{\beta} \ln(\alpha \cdot \beta) + \frac{1}{\beta} \ln t \tag{13}$$

The order in which the kinetics of the reaction biosorption process followed in relation to the R^2 values was PSO > PFO > Elovich. The R^2 value of the PSO was determined as 0.98, and the k_2 value was determined as 0.002 mg/g min. Additionally, this result confirmed that the biosorption process was chemical [57, 58].

Table 2 Comparison of q_{max} values in adsorption of safranin dyes with various sorbents

Biosorbent	q_{max} (mg/g)	Dye	Contact time	References
Modified red mud	89.4	Safranin O	90 min	37
<i>Lolium perenne</i> seeds	322.58	Safranin T	60 min	40
Lignin NPs	99	Safranin O	100 min	47
Lignin NPs-g-polyacrylic acid	138.8	Safranin O	100 min	47
<i>S. griseus</i> S15	188.67	Safranin O	1440 min	This study

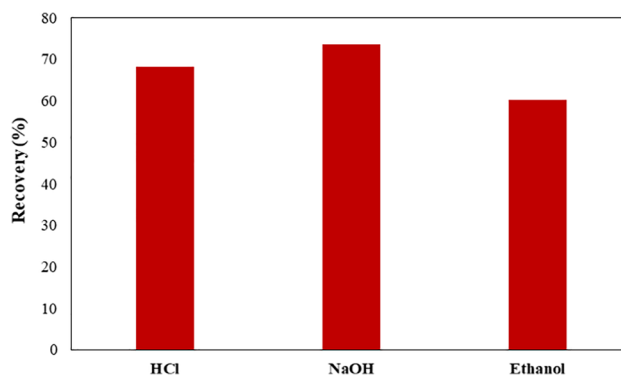


Fig. 11 Desorption of safranin O with different solvents (C_o , 200 mgL⁻¹; m , 50 mg; temperature, 25 °C, time, 24 h)

3.2.5 Biosorption thermodynamics

The effect of temperature on the biosorption was investigated at 5, 25, and 45 °C, and enthalpy energy (ΔH , kJ/mol), entropy change (ΔS , kJ/mol K), and free energy change (ΔG , kJ/mol) were determined in Fig. 10, and Eqs. 14, 15, and 16. Using Van't Hoff equation (Eq. 15), $\ln K_c$ vs. $1/T$ values were defined and plotted in Fig. 10.

$$K_c = \frac{C_a}{C_e} \tag{14}$$

$$\ln K_c = \frac{\Delta S}{R} - \frac{\Delta H}{R} \cdot \frac{1}{T} \tag{15}$$

$$\Delta G = \Delta H - T\Delta S \tag{16}$$

K_c , the equilibrium constant; C_a , the amount of dye retained per unit mass of biosorbent (mg/g); C_e , unbound dye (mg/L); R , the ideal gas constant, 8.314 J/mol K; and T , temperature (K).

The ΔH and the ΔS values were -13.59 kJ/mol and -31.19 J/K mol, respectively. Negative ΔH indicated that the biosorption was exothermic. ΔG values were -22.2, -22.8, and -23.5 kJ/mol at 5, 25, and 45 °C, respectively. These results indicated that the interaction between S15 and safranin O dye occurred spontaneously [59, 60].

Q_{max} of the *S. griseus* S15 was compared with those of some other biosorbents (Table 2). Although the biosorbent

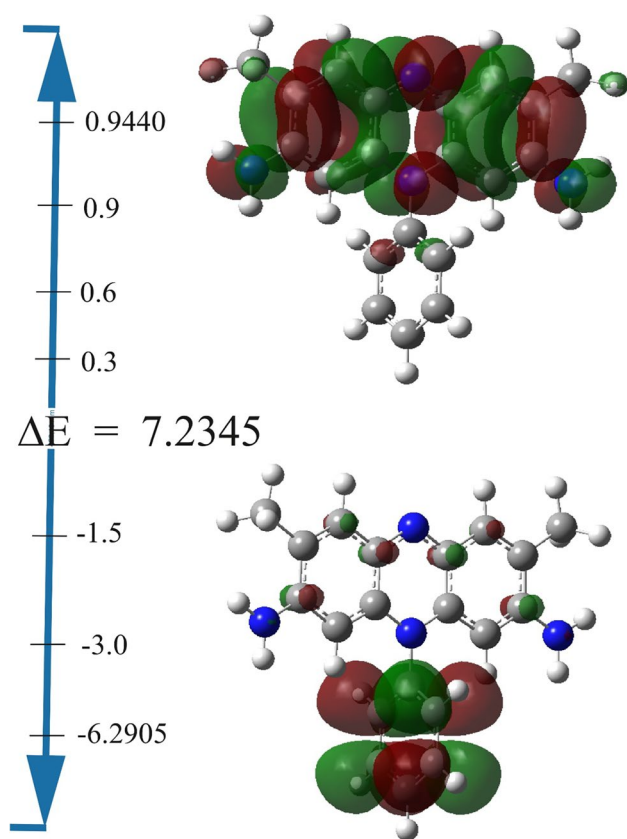


Fig. 12 A schematic representation of HOMO and LUMO of safranin O

was used without any treatment, it could be clearly seen that *S. griseus* S15 had a highest q_{\max} after the *Lolium perenne* seeds.

3.2.6 Desorption capacity

Reusability is an important biosorbent feature [56]. The final experiments constituted desorption of bound dye in different solvent environment: HCl, NaOH, and ethanol (Fig. 11). Desorption values were 68%, 74%, and 60% in HCl, NaOH, and ethanol solution, respectively. This result paves the way for the reusability of *S. griseus* S15.

3.3 Theoretical calculations

Theoretical calculations were performed to find and compare the activities of molecules, to determine their active sites, and to increase their activities [46]. The most important factor in determining the activities of molecules is to define the electron density of a molecule [61].

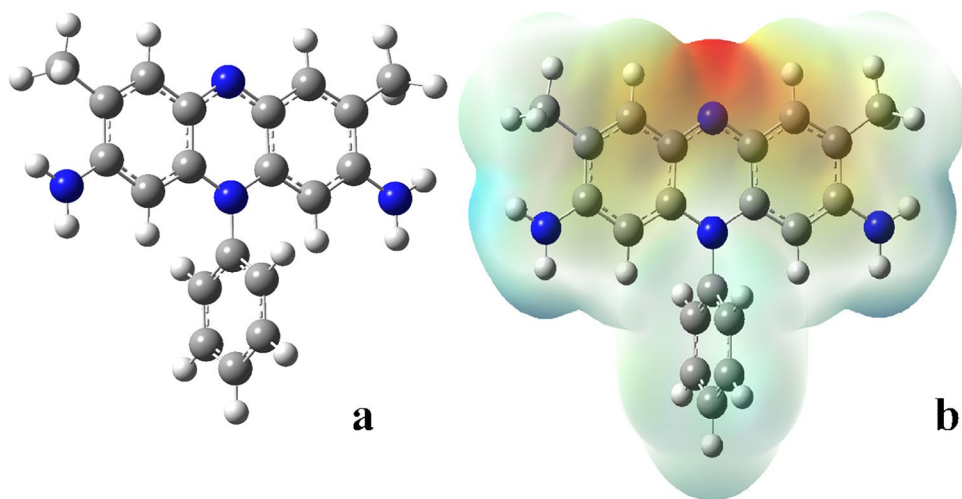
HOMO determines the electron-donating ability of the molecules in Fig. 12 [62]. A molecule with a higher HOMO will easily donate its electrons. LUMO values indicate the electron-accepting abilities of the molecules in Table 3 [63].

Another calculated parameter, ΔE , is known to yield high activity values for molecules with a low numerical value [64]. Electronegativity is the force of attraction of bond electrons of atoms in the molecule. Electronegativity values, similarly, are high for the molecules with the lowest numerical value [65].

Table 3 The calculated quantum chemical parameters of molecules

E_{HOMO}	E_{LUMO}	I	A	ΔE	η	μ	χ	ρ	ω	ε	dipol	Energy
B3LYP/6-31g level												
-3.1416	-0.4114	3.1416	0.4114	2.7301	1.3651	0.7326	1.7765	-1.7765	1.1560	0.8651	5.3956	-26,994.7866
B3LYP/6-31++g level												
-3.4915	-0.8452	3.4915	0.8452	2.6463	1.3232	0.7558	2.1684	-2.1684	1.7767	0.5628	5.3075	-26,995.8364
B3LYP/6-31++g** level												
-3.6243	-0.9241	3.6243	0.9241	2.7002	1.3501	0.7407	2.2742	-2.2742	1.9154	0.5221	4.7844	-27,003.6076
HF/3-21g level												
-6.1025	3.5922	6.1025	-3.5922	9.6947	4.8473	0.2063	1.2551	-1.2551	0.1625	6.1539	3.8910	-26,818.5923
HF/6-31g level												
-6.2905	0.9440	6.2905	-0.9440	7.2345	3.6172	0.2765	2.6733	-2.6733	0.9878	1.0123	3.7350	-26,819.2726
HF/SDD level												
-6.3757	0.9282	6.3757	-0.9282	7.3039	3.6519	0.2738	2.7237	-2.7237	1.0157	0.9845	3.4542	-26,830.4155
M062X/3-21g level												
-4.2521	0.5823	4.2521	-0.5823	4.8344	2.4172	0.4137	1.8349	-1.8349	0.6964	1.4359	5.3462	-26,983.8746
M062X/6-31g level												
-4.5403	-0.2890	4.5403	0.2890	4.2513	2.1256	0.4704	2.4146	-2.4146	1.3714	0.7292	5.2596	-26,984.7412
M062X/SDD level												
-4.6499	-0.3053	4.6499	0.3053	4.3446	2.1723	0.4603	2.4776	-2.4776	1.4129	0.7078	4.7911	-26,991.8422

Fig. 13 A schematic representation of the optimize structure (a) and ESP of safranin O (b)



Many quantum parameters of the molecules were calculated, and some of the results were presented visually in Fig. 13. ESP (electrostatic potential) map of the molecules yields information about the electron density in the molecule. The red-colored regions, indicating the presence of heteroatoms, are electron-rich regions. On the other hand, the blue-colored regions with carbon and hydrogen atoms in general, are the electron-poor regions [61].

It is possible to comment on the activity by molecular docking calculations of molecules with various biological materials. These calculations predict the active sites of molecules, the interaction sites of molecules, and the interactions with the proteins of bioadsorbent [62]. The most important factor that determines the activities

of molecules with molecular docking calculations is the interaction between molecules and proteins. More interaction means more inhibition. For this reason, the chemical interactions, involving hydrogen bonds, polar and hydrophobic interactions, π - π bonds, between the molecule and the protein become important in Figs. 14 and 15 [63].

The activities of the molecule against various proteins were compared Table 4. In the comparisons, the docking score parameter was determined on the basis of its numerical value. The most negative numerical value indicates the highest activity. Besides, Glide ligand efficiency, Glide hbond, Glide evdw, and Glide ecoul numerical values indicate interactions between dye molecules and proteins [46, 62].

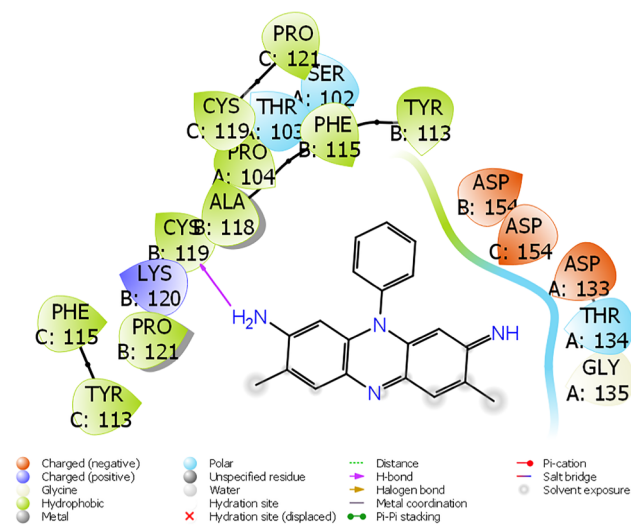


Fig. 14 Interactions of afzelin with bacterium *Streptomyces sp*

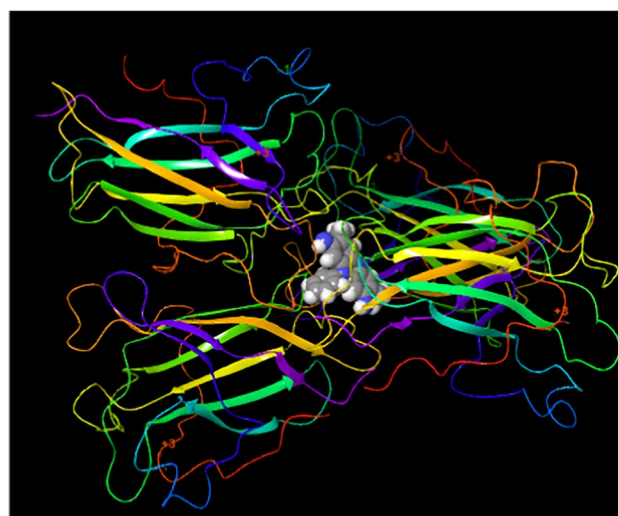


Fig. 15 Presentation interactions of afzelin with hCA I enzyme

Table 4 Numerical values of all docking parameters

	Streptomyces sp.
Docking score	-5.71
Glide ligand efficiency	-0.24
Glide hbond	0.00
Glide evdw	-30.50
Glide ecoul	-1.89
Glide emodel	-41.40
Glide energy	-32.39
Glide einternal	2.60
Glide posenum	377

Comparing the interactions of safranin O by ADME/T with various cellular proteins theoretically enabled us to predict whether this dye could have a drug potential in Table 5. The entry of the molecule into human metabolism implicates many processes including movements in metabolism and excretion from metabolism.

There are parameters useful in examining the chemical properties of molecules: mol_MW (mole mass of molecules), dipole (dipole moment), SASA (solvent accessible surface area), volume (molecule volume), donorHB and acptHB (number of hydrogen bonds that a molecule receives and gives off) [66]. In addition, there are also many parameters that examine the biological properties of molecules: QPlogHERG (Predicted IC₅₀ value for blockage of HERG K⁺ channels), QPPCaco and QPPMDCK (blood-brain and blood-bowel barriers), QPlogKp (predicted skin permeability), QPlogKhsa (prediction of binding to human serum albumin), and HumanOralAbsorption (predicted qualitative human oral absorption) [67].

4 Conclusion

The main aim of the study was to evaluate the biosorption potential of safranin O dye. For this purpose, *S. griseus* S15 isolated from the soil was used in biosorption experiments, and it was determined that the selected bacterial strain effectively removed safranin O dye. It was also concluded that *S. griseus* S15 biomass was a successful biosorbent in the biosorption of safranin O dye. The calculations show that the results of both Gaussian software calculations and molecular docking calculations of the molecule provide information about the active site of the molecule and many chemical and biological properties. When the ADME/T calculations made later are examined to apply the molecules to human metabolism, it is seen that the molecules meet the desired

Table 5 ADME properties of molecule

	Molecule	Reference range
mol_MW	314	130–725
dipole (D)	7.7	1.0–12.5
SASA	591	300–1000
FOSA	166	0–750
FISA	115	7–330
PISA	310	0–450
WPSA	0	0–175
volume (A ³)	1028	500–2000
donorHB	2.5	0–6
acptHB	3.5	2.0–20.0
glob (Sphere =1)	0.8	0.75–0.95
QPpolrz (A ³)	36.7	13.0–70.0
QPlogPC16	11.3	4.0–18.0
QPlogPoct	18.4	8.0–35.0
QPlogPw	10.7	4.0–45.0
QPlogPo/w	3.5	-2.0–6.5
QPlogS	-5.2	-6.5–0.5
CIQPlogS	-5.2	-6.5–0.5
QPlogHERG	-5.7	*
QPPCaco (nm/s)	803	**
QPlogBB	-0.7	-3.0–1.2
QPPMDCK (nm/s)	390	**
QPlogKp	-2.4	Kp in cm/h
IP (ev)	7.7	7.9–10.5
EA (eV)	1.0	-0.9–1.7
#metab	4	1–8
QPlogKhsa	0.5	-1.5–1.5
Human Oral Absorption	3	-
Percent Human Oral Absorption	100	***
PSA	62	7–200
RuleOfFive	0	Maximum is 4
RuleOfThree	0	Maximum is 3
Jm	0.0	-

*Concern below -5

**<25 is poor and >500 is great

***<25% is poor and >80% is high

conditions. The results obtained will be an important guide for many future studies.

Acknowledgements The numerical calculations reported in this paper were fully/partially performed at TUBITAK ULAKBIM, High Performance and Grid Computing Center (TRUBA resources).

Author contribution **MSÇ**: investigation, validation, writing—review and editing. **NK**: resources, investigation, writing—review and editing. **AFY**: methodology, writing—review and editing. **SÇ**: conceptualization, supervision, writing—original draft. **BT**: conceptualization, supervision, writing—review and editing.

Funding This work was supported by the Scientific Research Project Fund of Sivas Cumhuriyet University (CUBAP) under the project number RGD-020.

Data availability All data that support the results of this research are available within the manuscript.

Declarations

Ethical approval Not applicable.

Competing interests The authors declare no competing interests

References

- Lu SL (2016) Has the political influence of the US textile industry waned? A case study on the negotiation results of the trans-pacific partnership (TPP). In: International Textile and Apparel Association Annual Conference Proceedings 73:1
- Starovoitova D, Odido D (2014) Assessment of toxicity of textile dyes and chemicals via materials safety data sheets. *BioSciences* 9:241–248
- Qi X, Wu L, Su T, Zhang J, Dong W (2018) Polysaccharide-based cationic hydrogels for dye adsorption. *Colloids Surf B: Biointerfaces* 170:364–372
- Qi X, Zeng Q, Tong X, Su T, Xie L, Yuan K et al (2021) Polydopamine/montmorillonite-embedded pullulan hydrogels as efficient adsorbents for removing crystal violet. *J Hazard Mater* 402:123359
- Chequer FMD, de Oliveira GAR, Ferraz ERA, Cardoso JC, Zanoni MVB, de Oliveira DP (2013). Textile dyes: dyeing process and environmental impact. In: *Eco-friendly textile dyeing and finishing*. InTech. <https://doi.org/10.5772/53659>
- Yagub MT, Sen TK, Afroze S, Ang HM (2014) Dye and its removal from aqueous solution by adsorption: a review. *Adv Colloid Interf Sci* 209:172–184
- Morin-Crini N, Winterton P, Fourmentin S, Wilson LD, Fenyvesi É, Crini G (2017) Water-insoluble β -cyclodextrin-epichlorohydrin polymers for removal of pollutants from aqueous solutions by sorption processes using batch studies: a review of inclusion mechanisms. *Prog Poly Sci* 78:1–23
- Qi X, Wei W, Su T, Zhang J, Dong W (2018) Fabrication of a new polysaccharide-based adsorbent for water purification. *Carbohydr Polym* 195:368–377
- Holkar CR, Jadhav AJ, Pinjari DV, Mahamuni NM, Pandit AB (2016) A critical review on textile wastewater treatments: possible approaches. *J Environ Manag* 182:351–366
- Ranade VV, Bhandari VM (2014) Industrial wastewater treatment, recycling and reuse: an overview. *Ind Wastew Treat Recycl Reuse*:1. <https://doi.org/10.1016/C2012-0-06975-X>
- Abidi N, Errais E, Duplay J, Berez A, Jrad A, Schäfer G, Ghazi M, Semhi K, Trabelsi- Ayadi M (2015) Treatment of dye-containing effluent by natural clay. *J Clean Prod* 86:432–440
- Sahu O, Singh N (2019) Significance of bioadsorption process on textile industry wastewater. In: *The impact and prospects of green chemistry for textile technology*. Woodhead Publishing, pp 367–416
- Oller I, Malato S, Sánchez-Pérez J (2011) Combination of advanced oxidation processes and biological treatments for wastewater decontamination—a review. *Sci Total Environ* 409(20):4141–4166
- Singh K, Arora S (2011) Removal of synthetic textile dyes from wastewaters: a critical review on present treatment technologies. *Crit Rev Environ Sci Technol* 41(9):807–878
- Sarayu K, Sandhya S (2012) Current technologies for biological treatment of textile wastewater—a review. *Appl Biochem Biotechnol* 167(3):645–661
- Vijayaraghavan K, Yun Y-S (2008) Bacterial biosorbents and biosorption. *Biotechnol Adv* 26:266–291
- Volesky B (2007) Biosorption and me. *Water Res* 41:4017–4029
- Aksu Z (2005) Application of biosorption for the removal of organic pollutants: a review. *Process Biochem* 40:997–1026
- Park D, Yun YS, Park JM (2010) The past, present, and future trends of biosorption. *Biotechnol Bioprocess Eng* 15:86–102
- Ikram M, Zahoor M, Batiha GES (2020) Biodegradation and decolorization of textile dyes by bacterial strains: a biological approach for wastewater treatment. *Z Phys Chem* 235:1381–1393
- Pinheiro LRS, Gradissimo DG, Xavier LP, Santos AV (2022) Degradation of azo dyes: bacterial potential for bioremediation. *Sustainability* 14:1510
- Lade H, Govindwar S, Paul D (2015) Mineralization and detoxification of the carcinogenic azo dye Congo red and real textile effluent by a polyurethane foam immobilized microbial consortium in an upflow column bioreactor. *Int J Environ Res Public Health* 12:6894–6918
- Khan AU, Zahoor M, Rehman MU, Shah AB, Zekker I, Khan FA, Ullah R, Albadrani GM, Bayram R, Mohamed HRH (2022) Biological mineralization of methyl orange by *Pseudomonas aeruginosa*. *Water* 14:1551
- Ikram M, Naeem M, Zahoor M, Rahim A, Hanafiah MM, Oye-kanmi AA, Sadiq A (2022) Biodegradation of azo dye methyl red by *Pseudomonas aeruginosa*: optimization of process conditions. *Int J Environ Res Public Health* 19(16):9962
- Amin DH, Abdallah NA, Abolmaaty A, Tolba S, Wellington EMH (2020) Microbiological and molecular insights on rare Actinobacteria harboring bioactive prospective. *Bull Natl Res Cent* 44:1–12
- Subramani R, Sipkema D (2019) Marine rare actinomycetes: a promising source of structurally diverse and unique novel natural products. *Mar Drugs* 17:249
- Bagewadi ZK, Vernekar AG, Patil AY, Limaye AA, Jain VM (2011) Biodegradation of industrially important textile dyes by actinomycetes isolated from activated sludge. *Biotechnol Bioinf* 1:351–360
- Chalkha M, el Hassani AA, Nakkabi A, Tüzün B, Bakhouch M, Benjelloun AT, El Yazidi M (2023) Crystal structure, Hirshfeld surface and DFT computations, along with molecular docking investigations of a new pyrazole as a tyrosine kinase inhibitor. *J Mol Struct* 1273:134255
- Becke AD (1992) Density functional thermochemistry. I. The effect of the exchange only gradient correction. *J Chem Phys* 96(3):2155–2160. <https://doi.org/10.1063/1.462066>
- Vautherin D, Brink DT (1972) Hartree-Fock calculations with Skyrme's interaction. I. Spherical nuclei. *Phys Rev C* 5(3):626. <https://doi.org/10.1103/PhysRevC.5.626>
- Hohenstein EG, Chill ST, Sherrill CD (2008) Assessment of the performance of the M05–2X and M06–2X exchange-correlation functionals for noncovalent interactions in biomolecules. *J Chem Theory Comput* 4(12):1996–2000
- Bianchetti CM, Harmann CH, Takasuka TE, Hura GL, Dyer K, Fox BG (2013) Fusion of dioxygenase and lignin-binding domains in a novel secreted enzyme from cellulolytic *Streptomyces* sp. SirexAA-E. *J Biol Chem* 288(25):18574–18587
- Ghosh I, Kar S, Chatterjee T, Bar N, Das SK (2021) Adsorptive removal of Safranin-O dye from aqueous medium using coconut coir and its acid-treated forms: adsorption study, scale-up design, MPR and GA-ANN modeling. *Sustain Chem Pharm* 19:100374
- Çetinkaya S (2021) A novel isolate (S15) of *Streptomyces griseobrunneus* produces 1-dodecanol. *Curr Microbiol* 78(1):144–149
- Çetinkaya S, Kaya S, Aksu A, Çetintaş Hİ, Jalbani NS, Erkan S, Marzouki R (2023) Equilibrium and DFT modeling studies for the

- biosorption of Safranin O dye from water samples using *Bacillus subtilis* biosorbent. *J Mol Struct* 1276:134761
36. Çetinkaya HF, Cebeci MS, Kaya S, Jalbani NS, Maslov MM, Marzouki R (2022) Removal of erythrosine B dye from wastewater using chitosan boric acid composite material: experimental and density functional theory findings. *J Phys Org Chem* e4400. <https://doi.org/10.1002/poc.4400>
 37. Colak F, Atar N, Yazicioglu D, Olgun A (2011) Biosorption of lead from aqueous solutions by *Bacillus* strains possessing heavy-metal resistance. *Chem Eng J* 173:422–428
 38. Çetinkaya S, Eyupoglu V, Çetintaş Hİ, Yenidünya AF, Kebabcı Ö, Tüzün B (2023) Removal of Erythrosine B dye from wastewater by *Penicillium italicum*: experimental, DFT, and molecular docking studies. *J Biomol Struct Dyn*:1–12. <https://doi.org/10.1080/07391102.2023.2186704>
 39. Dennington R, Keith TA, Millam JM (2016) GaussView 6.0. 16. Semichem Inc.: Shawnee Mission, KS, USA
 40. Frisch MJ, Trucks GW, Schlegel HB, Scuseria GE, Robb MA, Cheeseman JR, Scalmani G, Barone V, Mennucci B, Petersson GA, Nakatsuji H, Caricato M, Li X, Hratchian HP, Izmaylov AF, Bloino J, Zheng G, Sonnenberg JL, Hada M et al (2009) Gaussian 09, revision D.01. Gaussian Inc, Wallingford CT
 41. Shahzadi I, Zahoor AF, Tüzün B, Mansha A, Anjum MN, Rasul A, Mojzych M (2022) Repositioning of acefylline as anti-cancer drug: synthesis, anticancer and computational studies of azomethines derived from acefylline tethered 4-amino-3-mercapto-1, 2, 4-triazole. *Plos one* 17(12):e0278027
 42. Zarrouk A, Hammouti B, Lakhlifi T, Traisnel M, Vezin H, Bentiss F (2015) New 1H-pyrrole-2, 5-dione derivatives as efficient organic inhibitors of carbon steel corrosion in hydrochloric acid medium: electrochemical, XPS and DFT studies. *Corros Sci* 90:572–584
 43. Schrödinger R (2021) Maestro. Schrödinger, LLC, New York, NY, pp 2021–2023
 44. Schrödinger R (2019) Protein preparation Wizard; Epik, Schrödinger, LLC, New York, NY, 2016; Impact, Schrödinger, LLC, New York, NY, 2016; Prime. Schrödinger, LLC, New York, NY, pp 2019–2014
 45. Schrödinger R (2021) LigPrep. Schrödinger, LLC, New York, NY, pp 2021–2023
 46. Tapera M, Kekeçmuhammed H, Tüzün B, Sarıpınar E, Koçyiğit ÜM, Yıldırım E, Zorlu Y (2022) Synthesis, carbonic anhydrase inhibitory activity, anticancer activity and molecular docking studies of new imidazolyl hydrazone derivatives. *J Mol Struct* 1269:133816
 47. Schrödinger R (2021) QikProp. Schrödinger, LLC, New York, NY, pp 2021–2023
 48. Sahu MK, Patel RK (2015) Removal of safranin-O dye from aqueous solution using modified red mud: kinetics and equilibrium studies. *RSC Adv* 5(96):78491–78501
 49. Sahu MK, Sahu UK, Patel RK (2015) Adsorption of safranin-O dye on CO₂ neutralized activated red mud waste: process modelling, analysis and optimization using statistical design. *RSC Adv* 5(53):42294–42304
 50. Moon SA, Salunke BK, Saha P, Deshmukh AR, Kim BS (2018) Comparison of dye degradation potential of biosynthesized copper oxide, manganese dioxide, and silver nanoparticles using *Kalopanax pictus* plant extract. *Korean J Chem Eng* 35(3):702–708
 51. Karadeniz SC, Isik B, Ugraskan V, Cakar F (2022) Agricultural *Lolium perenne* seeds as a low-cost biosorbent for Safranin T adsorption from wastewater: Isotherm, kinetic, and thermodynamic studies. *Phys Chem Earth Parts A/B/C*. <https://doi.org/10.1016/j.pce.2022.103338>
 52. Kamel MM, Alsohaimi IH, Alhumaimess MS, Hassan H, Alshammari MS, El-Sayed MY (2021) A glassy polyvinyl alcohol/silica gel hybrid composite for safranin removal: adsorption, kinetic and thermodynamic studies. *Res Chem Intermed* 47(3):925–944
 53. Antonova-Nikolova S, Stefanova V, Yocheva L (2006) Taxonomic study of *Streptomyces* sp. strain 34-1. *J Culture Collect* 5(1):10–15
 54. Maurya NS, Mittal AK (2013) Removal mechanism of cationic dye (Safranin O) from the aqueous phase by dead macro fungus biosorbent. *Water Sci Technol* 68(5):1048–1054
 55. Ali F, Ali N, Bibi I, Said A, Nawaz S, Ali Z, Salman SM, Iqbal HMN, Bilal M (2020) Adsorption isotherm, kinetics and thermodynamic of acid blue and basic blue dyes onto activated charcoal. *Case Stud Chem Environ Eng* 2:100040
 56. Verma M, Tyagi I, Kumar V, Goel S, Vaya D, Kim H (2021) Fabrication of GO–MnO₂ nanocomposite using hydrothermal process for cationic and anionic dyes adsorption: kinetics, isotherm, and reusability. *J Environ Chem Eng* 9(5):106045
 57. Banisheykholeslami F, Hosseini M, Darzi GN (2021) Design of PAMAM grafted chitosan dendrimers biosorbent for removal of anionic dyes: adsorption isotherms, kinetics and thermodynamics studies. *Int J Biol Macromol* 177:306–316
 58. Azimvand J, Didehban K, Mirshokraie SA (2018) Safranin-O removal from aqueous solutions using lignin nanoparticle-g-polyacrylic acid adsorbent: synthesis, properties, and application. *Adsorpt Sci Technol* 36(7-8):1422–1440
 59. Isik B, Ugraskan V, Cankurtaran O (2022) Effective biosorption of methylene blue dye from aqueous solution using wild macrofungus (*Lactarius piperatus*). *Sep Sci Technol* 57(6):854–871
 60. Okumuş ZÇ, Doğan TH (2019) Biyodizeldeki suyun reçine ile uzaklaştırılması: adsorpsiyon izotermi, kinetiği ve termodinamik incelemesi. *Avrupa Bilim ve Teknoloji Dergisi* 15:561–570
 61. Sayın K, Ataseven H (2023) Structural, electronic, ADME and p450 analyses of boron containing compounds against omicron variant (B. 1.1. 529) in SARS-CoV-2. *Cumhuriyet Sci J* 44(1):72–80
 62. Poustforoosh A, Farmariz S, Nematollahi MH, Hashemipour H, Pardakhty A (2022) Construction of bio-conjugated nano-vesicles using non-ionic surfactants for targeted drug delivery: a computational supported experimental study. *J Mol Liq* 367:120588
 63. Poustforoosh A, Hashemipour H, Pardakhty A, Pour MK (2022) Preparation of nano-micelles of meloxicam for transdermal drug delivery and simulation of drug release: a computational supported experimental study. *Can J Chem Eng* 100(11):3428–3436
 64. Stanger FV, Dehio C, Schirmer T (2014) Structure of the N-terminal gyrase B fragment in complex with ADP. Pi reveals rigid-body motion induced by ATP hydrolysis. *PloS one* 9(9):e107289
 65. Naghiyev F, Mamedov I, Askerov R, Taslimi P, Poustforoosh A (2022) Synthesis and biological activity of functionally substituted pyrimidine and pyran derivatives on the basis of isatylidene malononitriles. *ChemistrySelect* 7(33):e202202006
 66. Poustforoosh A, Hashemipour H, Tüzün B, Azadpour M, Farmariz S, Pardakhty A, Nematollahi MH (2022) The impact of D614G mutation of SARS-COV-2 on the efficacy of anti-viral drugs: a comparative molecular docking and molecular dynamics study. *Curr Microbiol* 79(8):241
 67. Adenan NH, Lim YY, Ting ASY (2022) Removal of triphenylmethane dyes by *Streptomyces bacillaris*: a study on decolorization, enzymatic reactions and toxicity of treated dye solutions. *J Environ Manage* 318:115520

Publisher's note Springer Nature remains neutral with regard to jurisdictional claims in published maps and institutional affiliations.

Springer Nature or its licensor (e.g. a society or other partner) holds exclusive rights to this article under a publishing agreement with the author(s) or other rightsholder(s); author self-archiving of the accepted manuscript version of this article is solely governed by the terms of such publishing agreement and applicable law.